Chemical Physics 375 (2010) 1–7

Contents lists available at ScienceDirect

Chemical Physics

journal homepage: www.elsevier.com/locate/chemphys

Correlation between structural studies and third order NLO properties of selected new quinolinium semi-organic compounds

K. Bouchouit [a,*], E.E. Bendeif [b], H. EL Ouazzani [c], S. Dahaoui [b], C. Lecomte [b], N. Benali-cherif [d], B. Sahraoui [c]

[a] Département de Chimie, Faculté des Sciences, Université de Jijel, Algeria
[b] Laboratoire de Cristallographie, Résonance Magnétique et Modélisation CRM^2 CNRS UMR 7036, Institut Jean Barriol, Nancy Université, Faculté des Sciences, BP 239, 54506 Vandœuvre-lès-Nancy, CEDEX, France
[c] Institut des Sciences et Technologies Moléculaires d'Angers UMR CNRS 6200 MOLTECH ANJOU, Université d'Angers 2, Boulevard Lavoisier, 49045 Angers, France
[d] Laboratoire des Structures, Propriétés et Interactions Inter Atomiques (LASPI2A), Centre Universitaire de Khenchela, 40000 Khenchela, Algeria

ARTICLE INFO

Article history:
Received 11 May 2010
In final form 7 July 2010
Available online 13 July 2010

Keywords:
Single crystal X-ray diffraction
Structural characterization
Nonlinear optics
Semi-organic compounds
Thin films
THG
DFWM

ABSTRACT

New quinolinium semi-organic compounds of formula $(C_9H_8N)_2^+ \cdot SO_4^{2-}$, H_2O (**I**) (bis-quinolinium sulphate monohydrate) and $(C_9H_8N)^+ \cdot NO_3^-$ (**II**) (quinolinium nitrate) have been synthesized and characterized by UV–Vis absorption spectroscopy, nonlinear optical (NLO) measurements and by single crystal X-ray diffraction. The third order nonlinear optical properties of (**I**) and (**II**) were investigated using two methods: the degenerate four wave mixing technique (DFWM) performed in solution at $\lambda = 532$ nm and the third-harmonic generation (THG) measurements carried out on thin films at $\lambda = 1064$ nm. The NLO measurements showed that compound (**I**) presents better nonlinear optical properties compared to compound (**II**). To understand further the optical behaviour of (**I**) and (**II**), the crystal structures of both compounds were determined from accurate single crystal X-ray diffraction measurements performed at 100 K. The crystallographic studies revealed the key role of the intermolecular interactions and the molecular arrangements in the enhancement of the NLO properties.

1. Introduction

In recent years there has been growing interest in molecular nonlinear optical materials due to their high potential for optoelectronic and photonic applications [1,2]. The molecular nature of the materials offers considerable design possibilities which should permit to scale up the favourable molecular nonlinear optical properties to macroscopic devices [3–8]. Organic nonlinear optical materials with aromatic rings represent a large class of such materials with high nonlinearity, fast response and high optical damage threshold [9–11]. However, their use for applications is limited by their rather poor mechanical and thermal stabilities and the lack of sufficiently large single crystals of optical quality. Organic–inorganic hybrid materials are expected to perform better in this. Especially semi-organic materials with a non-centrosymmetric cell, large polarizabilities and nonlinear optical coefficients are currently intensively investigated [12–19]. A variety of semi-organic crystals for nonlinear optical applications has been developed, amongst them compounds with organic cations and inorganic or organic anions [20].

Recently, we have reported on the origin of the nonlinear optical response showing that the nonlinear susceptibility of third-harmonic generation is related not only to the number of the π-conjugated systems but also to the following factors: solvent molecule effects and hydrogen bonds interactions that generate partial charges on the hydrogen atoms which increase significantly the dipole moment of molecules [21,22].

In the present work, we report on a detailed study performed on two new quinolinium semi-organic compounds (bis-quinolinium sulphate monohydrate, $(C_9H_8N)_2^+ \cdot SO_4^{2-}$, H_2O and quinolinium nitrate, $(C_9H_8N^+)^+ \cdot NO_3^-$), displaying interesting NLO properties. The results of the degenerate four wave mixing (DFWM) experiments performed at 532 nm and the third-harmonic generation (THG) measurements carried out at 1064 nm of the studied compounds are presented and discussed. On the basis of the structural analysis, we show the important role of the intermolecular interactions and the molecular arrangement for the modification of the NLO properties.

2. Experimental details

2.1. Crystallization and sample preparation

The studied compounds were prepared by slow evaporation of quinoline (99%, Aldrich) solutions in nitric and sulfuric acid at room temperature. The obtained colourless crystals were washed with water and dried in air.

* Corresponding author.
E-mail address: karim.bouchouit@laposte.net (K. Bouchouit).

0301-0104/$ - see front matter © 2010 Elsevier B.V. All rights reserved.
doi:10.1016/j.chemphys.2010.07.007

For the DFWM experiments solutions of very low concentration ($c = 10^{-2}$ mol/l) were obtained by dissolving crystals in a gently heated aqueous solution. We also prepared thin films for the TGH measurements: a semi-organic layer was deposited on the top of glass (Chevallier S.A glasses) first, then the samples were dried in oven for 20 min at 120 °C. The resulting thin layers were then moved into the glove box (under inert atmosphere). Finally, semi-organic thin films were formed by slow evaporation (Joule effect). The current used for the evaporation process was 3 A at $4 \cdot 10^{-7}$ mbar.

2.2. UV spectra

The UV–Vis spectra of **I** and **II** are shown in Fig. 1. The measurements were performed in 1 cm (quartz) cell using a solution of low concentration ($c = 10^{-5}$ mol/l). The spectra clearly show that both compounds absorb in a small zone ranging from 250 nm to 350 nm. This absorption area can be attributed to the quinolinium aromatic moieties absorption bands.

2.3. X-ray diffraction

2.3.1. Data collection and reduction

The crystal structures of two new organic–inorganic salts, *i.e.* bis-quinolinium sulphate monohydrate, $(C_9H_8N)_2^+ \cdot SO_4^{2-}$, H_2O (**I**) and quinolinium nitrate, $(C_9H_8N)^+ \cdot NO_3^-$ (**II**) have been determined by single-crystal X-ray diffraction analysis. Single crystals of dimensions $0.20 \times 0.12 \times 0.10$ mm for (**I**) and $0.18 \times 0.15 \times 0.08$ mm for (**II**) were fixed on a glass fibre with silicon grease, mounted on the goniometer head of the Nonius Kappa CCD diffractometer equipped with a two-dimensional CCD detector and conventional X-ray tube (Mo Kα radiation, $\lambda = 0.71073$ Å). To decrease thermal smearing effects, the samples were cooled at 100(2) K with a liquid-nitrogen Oxford Cryostream cooling device using the cooling rate 120 K h^{-1}. The temperature was beforehand calibrated using a K-type Chromel–Alumel thermocouple positioned at the same place on the crystal. The crystal temperature was stable to within 2 K. Data collection was controlled by the program *COLLECT* [23]. The cell parameters were determined from an analysis of the Bragg peak positions collected on the same sets of 15 images. X-ray diffraction data were collected at a fixed detector position using ω step scans repeated at different values of the φ angle. Each frame covered a 1° omega rotation step. Coverage of reciprocal space was more than 99% complete to $(\sin\theta_{max}/\lambda)$ of 0.7 $Å^{-1}$ for both crystals. Final cell parameters were deduced from a least-squares post-refinement on all measured reflections. Interframe scaling using the intensity of equivalent reflections was checked and did not show any crystal decay during data collection, this scaling procedure was nevertheless applied.

The collected reflections were integrated with the *DENZO* program implemented in the *HKL2000* package [24]. The unit-cell parameters were refined by the program *SCALEPACK*, which is also part of the *HKL2000* package. Data reduction was performed with the program *SCALEPACK*. The absorption was small, but the data were nevertheless corrected by means of Gaussian numerical integration using the *ABSORB* program [25].

2.3.2. Crystal structures refinements

The structures were solved by direct methods and refined by full-matrix least-squares on F^2 using *SHELXL*97 [26] with no constraints applied. All calculations were carried out using the *WinGX* software package [27]. Atomic scattering factors were taken from the *International Tables for Crystallography* (1992, Vol. C, Tables 4.2.6.8 and 6.1.1.4). The displacement parameters of the non-H atoms were refined anisotropically using all reflections with $I > 2\sigma(I)$. The electron density of the H atoms was clearly identified in the Fourier difference maps, and their atomic coordinates and isotropic displacements parameters were refined. The full experimental details and refinements results for compound (**I**) and (**II**) are summarized in Table 1.

2.4. Nonlinear optical properties

2.4.1. DFWM measurements

Third order nonlinear optical susceptibilities $(\chi^{(3)})$ of **I** and **II** solutions were measured by the standard backward degenerate four wave mixing (DFWM) method using a Nd:YAG laser at $\lambda = 532$ nm with 30 ps pulses and 1 Hz repetition rate [28,29]. In

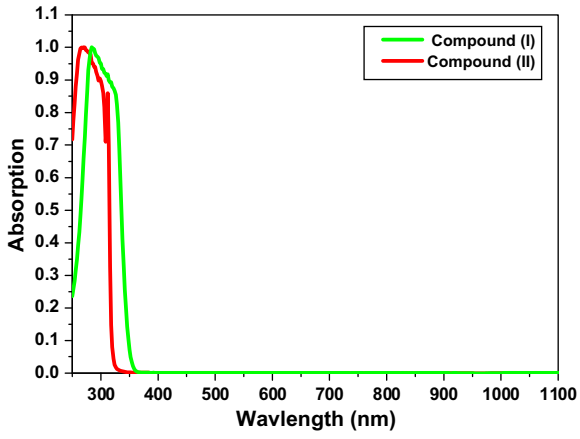

Fig. 1. The linear absorption spectra for compound **I** and **II**.

Table 1
Crystal data and structure refinement for **I** and **II**.

	I	II
Chemical formula	$C_{18}H_{18}N_2O_5S$	$C_9H_8N_2O_3$
Formula weight ($g\ mol^{-1}$)	374.40	192.17
Temperature (K)	100(2)	100(2)
Wavelength (Å)	0.71073	0.71073
Cell setting, space group	Triclinic, $P\bar{1}$	Monoclinic, $C2/c$
Unit cell dimensions	$a = 7.2660(10)$ Å, $\alpha = 88.382(9)°$	$a = 24.006(5)$ Å
	$b = 7.2830(10)$ Å, $\beta = 77.015(8)°$	$b = 3.6758(7)$ Å, $\beta = 99.96(3)°$
	$c = 15.6680(10)$ Å, $\gamma = 86.637(8)°$	$c = 19.154(4)$ Å
Volume ($Å^3$)	806.43(17)	1664.7(6)
Z	2	8
Calculated density ($Mg\ m^{-3}$)	1.542	1.534
μ (mm^{-1})	0.236	0.118
Absorption correction	Integration	Integration
T_{min}, Tmax	0.911, 0.946	0.938, 0.963
$F(0\,0\,0)$	392	800
Crystal size (mm)	$0.15 \times 0.12 \times 0.10$	$0.15 \times 0.12 \times 0.10$
Theta range for data collection	2.67–30°	2.74–30°
Limiting indices	$h = -10 \rightarrow 10$	$h = 0 \rightarrow 33$
	$k = -10 \rightarrow 0$	$k = 0 \rightarrow 5$
	$l = -21 \rightarrow 22$	$l = -26 \rightarrow 26$
Reflections collected	4678	2403
Parameters	235	159
Independent reflections ($I > 2\sigma(I)$)	3725 [R(int) = 0.068]	2153 [R(int) = 0.067]
Refinement method	Full-matrix least-squares on F^2	Full-matrix least-squares on F^2
Largest diffraction peak and hole	0.546 and −0.502 e $Å^{-3}$	0.463 and −0.362 e $Å^{-3}$

DFWM geometry, two strong, equally intense, counter-propagating pump beams and a weak probe beam were temporally and spatially overlapped in the sample. The probe beam makes a small angle ($\theta = 12°$) with respect to the pump beams and its intensity was adjusted at $I_{probe} = 6 \times 10^{-2} I_{pump}$. A phase-conjugated signal generated from these three laser beams of the same frequency (ω) was collected at the reverse direction of the probe beam. This signal was measured by a photomultiplier tube (PMT) and fed to a digital storage oscilloscope (Tektronix TDS 3054). A part of the input laser beam was split off and measured by a photodiode in order to monitor the input laser energies.

The studied compounds were dissolved in water in a 1 mm thick cuvette. We used carbon disulfide (CS_2) as a reference material to calibrate the DFWM measurements. The third order nonlinear optical susceptibility of CS_2 ($\chi^{(3)} = 1.94 \cdot 10^{-20}$ [m^2/V^2]) is in good agreement with the literature values.

The DFWM reflectivity (R) was calculated from the propagation equations of the interacting beams, which were deduced from the Maxwell equations using the approximation of slow amplitude variation and taking into account the linear and nonlinear absorption or only the linear absorption coefficients (Eq. (1)). The DFWM reflectivity (R) is defined as the total DFWM signal intensity divided by the incident probe-pulse intensity, is plotted as a function of the pump-pulse intensity (Fig. 2). The DFWM reflectivity (R) can be expressed as follows [28–30]:

$$R_{ijkl} = \frac{I^{(4)}(0)}{I^{(3)}(0)} = \begin{cases} \frac{p^2 + \frac{\alpha^2}{4}}{\left[p(\mathrm{ctg}(p\ell)) + \frac{\alpha}{2}\right]^2}, & p^2 \geqslant 0 \\ \frac{p^2 + \frac{\alpha^2}{4}}{\left[q(\mathrm{ctgh}(q\ell)) + \frac{\alpha}{2}\right]^2}, & p^2 < 0 \end{cases} \quad (1)$$

where $p^2 = \left(\frac{48\pi^3}{n^2 c\lambda}\chi^{(3)}_{ijkl}\right)^2 I^{(1)}(0)^2 \exp(-\alpha\ell) - \frac{\alpha^2}{4}$, $q = ip$ and the parameter ℓ is the cell length.

In order to characterise the individual molecule we determined the second order hyperpolarizability using the following relation:

$$\gamma = \chi^{(3)}(F^4 N)^{-1} \quad (2)$$

where $F = (n^2 + 2)/3$ is the Lorentz field factor correction, $N = N_A \cdot C/M$ is number of solved molecules per unit volume and N_A is Avogadro number.

2.4.2. THG measurements

Third order nonlinear optical susceptibility of the investigated compounds was also evaluated by THG measurements. The measurements were performed on thin films using a Q-switched Nd:YAG laser at $\lambda = 1064$ nm with 16 ps pulse, 10 Hz frequency and 1.6 mJ pulse power. A half wave plate has been placed between two polarizers in order to adjust the polarization and the power of the fundamental beam. The intensity at the input face of the sample is taken for being a Gaussian distribution in space and time. The beam diameter was 0.65 mm at the sample position and the applied power density was 2 GW/cm^2. The beam was focused on the sample passing through a lens ($f = 25$ cm). The films were mounted on a rotation stage. A 10 nm narrow line interferential filter (FL355) centred at 355 nm wavelength was used to block the pump beam before crossing the photodetector. We also used density attenuator to reduce the intensity generated from the nonlinear medium. The third harmonic signal was detected by photomultiplier tube (Model: Hamamatsu) which was integrated with a boxcar and processed by a computer. A portion of the input beam was selected and measured by a fast photodiode to monitor the input energy. Finally, we obtained the so-called Maker fringes [31] which were generated by rotating the sample in the range ±60° to the normal. We used SiO_2 as a reference material to calibrate the THG measurements. The third order nonlinear optical susceptibility of SiO_2 was determined to be $\chi^{(3)} = 2.00 \cdot 10^{-22}$ [m^2/V^2] in agreement with the literature values [32]. The intensity of the generated TH is given by the following formula [33,34]:

$$\chi^{(3)} = Cte \cdot \frac{A_3 I_{3\omega}}{A_1\{\exp[i3\omega l(N^{(2)}_{\omega} - N^{(2)}_{3\omega})/c] - 1\}} \quad (3)$$

$$A_1 = \frac{N^{(2)}_{3\omega} + N^{(2)}_{\omega}}{N^{(3)}_{3\omega} + N^{(2)}_{3\omega}}, \quad A_3 = 1 - \left(\frac{N^{(1)}_{3\omega} - N^{(2)}_{3\omega}}{N^{(1)}_{3\omega} + N^{(2)}_{3\omega}}\right)\left(\frac{N^{(3)}_{3\omega} - N^{(2)}_{3\omega}}{N^{(3)}_{3\omega} + N^{(2)}_{3\omega}}\right) e^{i6\omega N^{(2)}_{3\omega} l/c}$$

$$N^{j}_{\omega,3\omega} = n^{j}_{\omega,3\omega} \cos\theta^{j}_{\omega,3\omega}$$

where $n^{(j)}_{\omega;3\omega}$ is the refractive index of the jth medium corresponding to the fundamental frequency ω; 3ω, the frequency of the third harmonic signal and l, the film thickness. The $\chi^{(3)}$ is the third order nonlinear optical susceptibility of the film; $I_{3\omega}$, the power of the generated third harmonic signal and θ, the rotation angle.

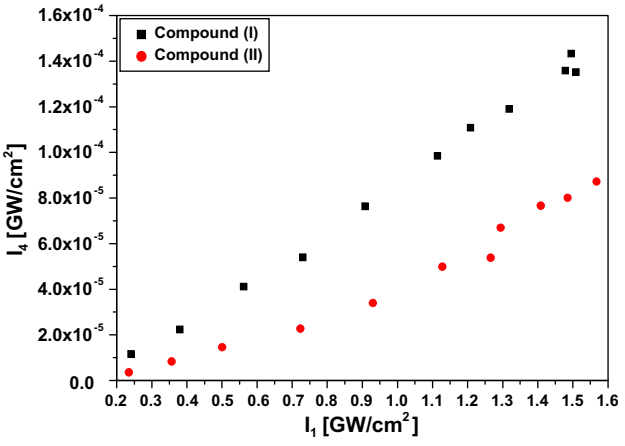

Fig. 2. The DFWM reflectivity (R) of bis-quinolinium sulphate hydrate and quinolinium nitrate as a function of input pump intensity.

3. Results and discussion

3.1. Structures and crystal packing

3.1.1. Bis-quinolinium sulphate monohydrate, $(C_9H_8N)_2^+ \cdot SO_4^{2-}$, H_2O (I)

The crystal structure of (**I**) (Fig. 3) can be described as being composed of chains of SO_4^{2-} groups and water molecules extending along the a-axis and alternating with $C_9H_8N^+$ quinolinium-stacked layers (Fig. 4). The asymmetric unit contains two quinolinium cation $(C_9H_8N)^+$, one sulphate anion $(SO_4)^{2-}$ and one water molecule. The inorganic chains and the quinolinium layers are connected through five interactions: *firstly via* two strong N–H···O hydrogen bonds (N1–H1n···O2 and N2–H2n···O4) and *secondly via* three weaker C–H···O intermolecular interactions (C17–H17···O2, C3–H3···O3 and C5–H5···O1w). The quinolinium entities are linked together by only aromatic π–π stacking interactions to form infinite perpendicular layers. The average spacing between the quinolinium molecules in the column is 3.332(2) Å. The water molecules play an important role in the three-dimensional network of hydrogen bonding. In fact, the water molecules act as bridges between the sulphate groups through two hydrogen bonds: (Ow1–H1w···O3 and O1w–H2w···O1). Besides these two hydrogen bonds, the water molecules are also connected to the quinolinium cations by a weaker (C5–H5···O1w) interaction. The intermolecular packing appears to be controlled by a three-dimensional network of N–H···O and C–H···O hydrogen bonds.

As discussed above, all the sulphate oxygen atoms are involved in hydrogen bonds: O1 and O4 are acceptors only once, while O2 and O3 are acceptor twice. One notices, first, that the sulphate

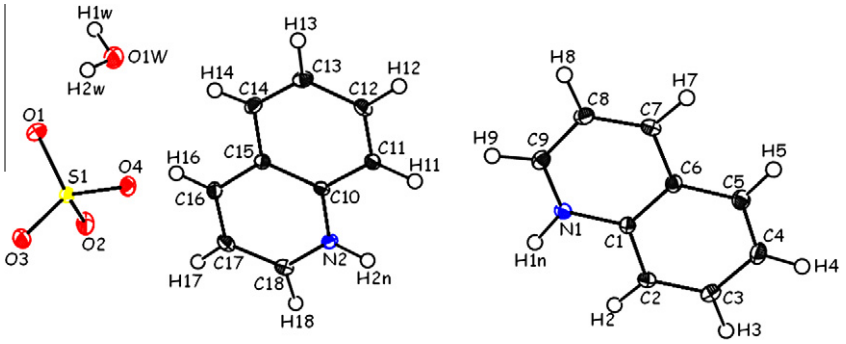

Fig. 3. Ortep III representation [35] of the bis-quinolinium sulphate monohydrate with thermal displacement ellipsoids plotted at 50% probability. H atoms are represented by spheres.

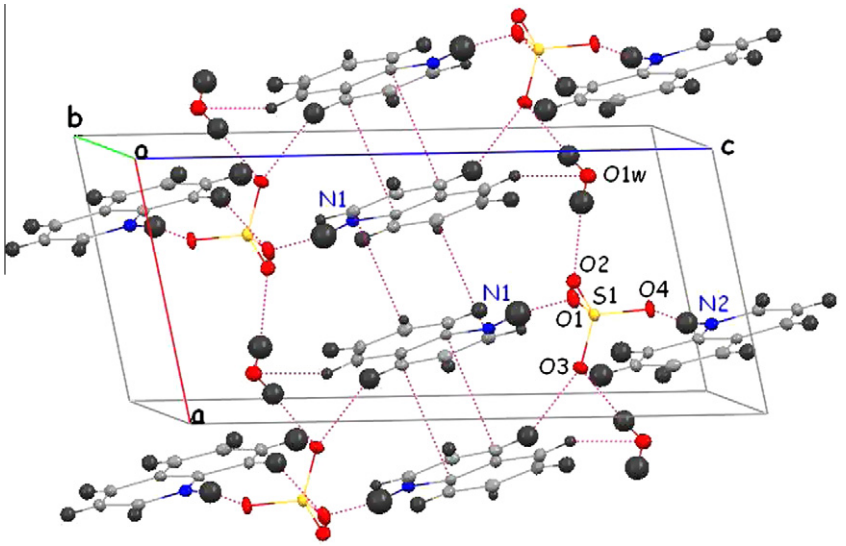

Fig. 4. View along the *b*-axis of the crystal parking of (**I**) showing the alternating $(C_9H_8N)_2^+ \cdot SO_4^{2-}$ and H_2O moieties.

anion has a distorted tetrahedral configuration. Inside the $(SO_4)^{2-}$ tetrahedron the S1–O2 [1.499(2) Å] and S1–O4 [1.485(2) Å] are longer (by ~0.027 and 0.013 Å, respectively) than S1–O1 [1.472(2) Å] and S1–O3 [1.472(2) Å]. These significant differences in S–O bond lengths are due to the fact that O2 and O4 are involved in strong hydrogen bonding (N1···O2: 2.550(3) Å and N2···O4: 2.626(3) Å) compared to that involving O1 and O3 (Ow1···O1: 2.875(3) Å and Ow1···O3: 2.837(3) Å).

Examining the interatomic distances and angles of the quinolinium cations in (**I**) shows that the majority of the bond lengths and angles found in (**I**) are fairly similar to those in the Quinoline molecule [36]. However, it is worth noting the enlargement of the C–N–C angle [121.9(2)° and 122.1(2)°] due to the capture of a proton, compared to the C–N–C angle in Quinoline [117.0(1)°] [36]. This protonation elongates the N–C bond lengths by ~0.01 Å (in average), and enlarges the C–N–C angle by about +5°. The benzene and the pyridinium rings are nearly coplanar and their deviation from the mean plane is only 1.53(2)°. The dihedral angle observed in the molecular structure of quinoline is 1.52(2)° [36].

3.1.2. *Quinolinium nitrate*, $(C_9H_8N)^+ \cdot NO_3^-$ (***II***)

The molecular structure of quinolinium nitrate is given in Fig. 5. In this structure one can observe NO_3^- anionic columns parallel to the *b*-axis surrounded by six quinolinium $(C_9H_8N)^+$ cationic groups. The molecular structure can be viewed as a donor–acceptor ad-

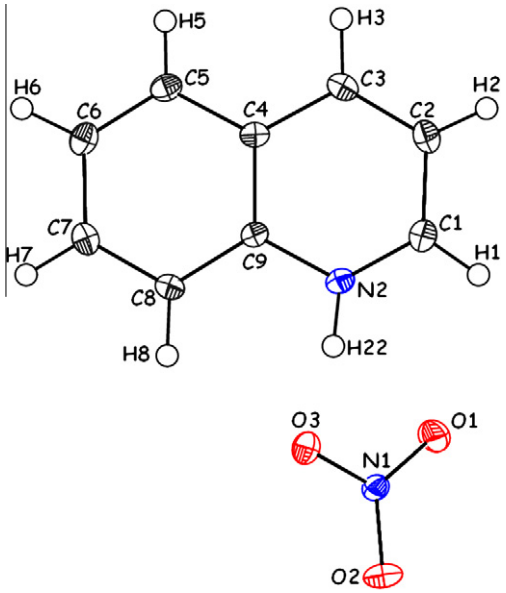

Fig. 5. Ortep III representation [35] of the quinolinium nitrate with thermal displacement ellipsoids plotted at 50% probability. H atoms are represented by spheres.

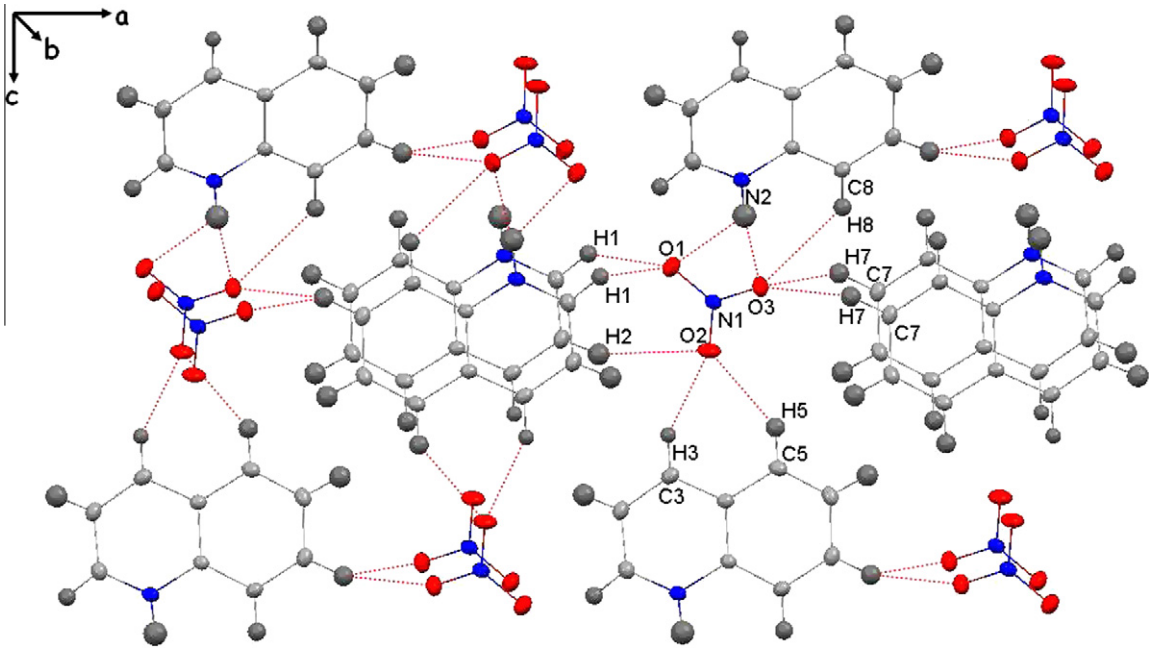

Fig. 6. The crystal structure parking of (**II**) viewed along the *b*-axis.

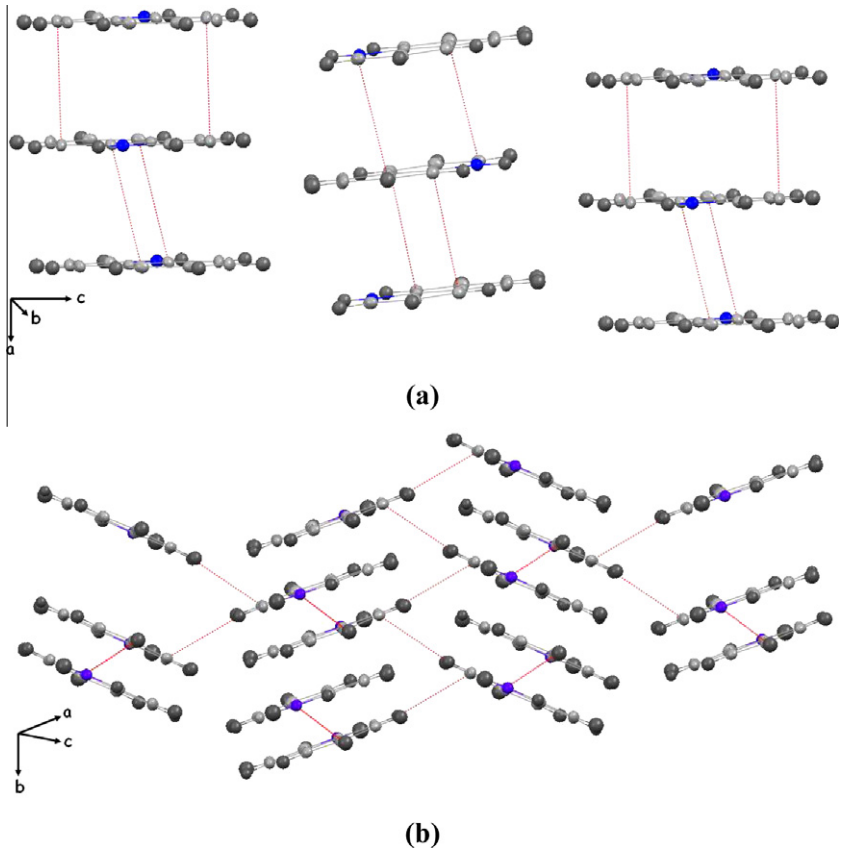

Fig. 7. Quinolinium molecules arrangement: (a) in (**I**) and (b) in (**II**).

duct, in which the nitrate anions and the quinolinium cations play an important role in the hydrogen bonding pattern (Fig. 6). Nevertheless this hydrogen bonding network does not point out any direct hydrogen-bond between the quinolinium cations.

The detailed geometry of the nitrate entities shows that the N1–O1 [1.253(2) Å] and N1–O2 [1.245(2) Å] bond lengths are significantly shorter than the N1–O3 bond [1.271(2) Å], which is in accordance with the relatively strong interaction involving the

Table 2
The third order NLO results obtained from THG experiments performed on thin films of compounds (**I**) and (**II**). (α) is the linear absorption coefficient m, ($\chi^{(3)}$) is the third order nonlinear optical susceptibilities. (γ) is the second order hyperpolarizability, ($\chi^{(3)}/\alpha$) is the factor of merit and $\left(\chi^{(3)}_{THG}\right)$ is the third order nonlinear optical.

Compounds	M [g/mol]	α [cm^{-1}]	$\chi^{(3)}_{exp}10^{20}$ [$m^2\ V^{-2}$]	$\gamma_{exp}10^{-43}$ [$m^5\ V^{-2}$]	$\chi^{(3)}_{exp}10^{20}\alpha$ [$m^3\ V^{-2}$]	$\chi^{(3)}_{THG}10^{20}$ [$m^2\ V^{-2}$]
I	374.40	0.250	0.98	4.85	3.92	1.68
II	192.17	0.472	0.71	1.80	1.50	0.56
CS_2	76.1	~0	1.94	–	4.71×10^{-2}	–

O3 atom with the imino group N2 atom of the pyridinium ring (N2–H22···O3) [2.741(3) Å]. On the other hand, the nitrate group acts as a hydrogen-bond acceptor from five neighboring quinolinium cations through a weak C–H···O interactions and ensure therefore the anion–cation connection along the *a*- and *c*-axes.

The geometrical features of the quinolinium cations are similar to those previously described in (**I**). The organic rings atoms are almost coplanar and the angle between the mean plane of the pyridinium and the benzene rings (*i.e.* the dihedral angle) is 1.15(2)° and this puckering along the C4–C9 bond is commonly found in quinolinium salts structures [36,37]. The presence of such puckering has already been noticed in compounds containing similar pyridinium rings [38]. The interplanar separation between quinolinium layers is 3.398(2) Å leading to a π–π stacking interactions between the cations as also observed in (**I**).

In summary the structural investigation shows that the inspection of hydrogen bonding network in both salts shows a direct hydrogen-bond interaction between the quinolinium cation and the sulphate (nitrate) anion. The (N–H···O) hydrogen bonds that connect the sulphate anions $(SO_4)^{2-}$ and the imino groups N1 and N2 atoms in (**I**) are strong, while those between the nitrate anions NO_3^- and the imino group N2 atom in (**II**) are of moderate strength. In addition to the π–π stacking interactions between the quinolinium layers, two categories of intermolecular interactions can be distinguished in both compounds: (N–H···O) and (C–H···O).

The benzene and pyridinium aromatic rings are almost coplanar in both salts with a slight difference in the dihedral angle. It is interesting to note that the molecular arrangement of the quinolinium cations in (**I**) is completely different to that observed in (**II**) (Fig. 7). While in (**I**) a parallel cationic layers arrangement is found (Fig. 7 a), the organic $(C_9H_8N)^+$ quinolinium moieties build a zigzag layers in (**II**) with a longer interlayer spacing (Fig. 7b).

3.2. NLO proprieties

The linear absorption coefficient (α) values of the investigated compounds were calculated from the relation $T = \exp(-\alpha L)$. Taking into account the absorption coefficients obtained from transmission experiment, the third order NLO properties of each compound were deduced from the DFWM modelled data (Fig. 2). The obtained results are summarized in Table 2. α, $\chi^{(3)}$, γ and $\chi^{(3)}/\alpha$ represent, respectively, the linear absorption coefficients, the susceptibilities of third order, the second order nonlinear hyperpolarisabilities value and the figure of merit ($\chi^{(3)}/\alpha$), which is an important parameter for optical or optoelectronic applications.

One can notice from Table 2 that the value of the third order nonlinear optical susceptibility ($\chi^{(3)}$) of compound (**I**) is three times larger than that observed in compound (**II**). Such a behaviour may be explained by the fact that the hydrogen-bond interactions in compound (**I**) are stronger than those in compound (**II**). Moreover, the molecular packing in compound (**I**) helps strengthen the donor–acceptor interactions and provides an appropriate pathway for intermolecular charge transfer leading to a significant enhancement of the NLO properties.

The second order nonlinear hyperpolarizability (γ) values ($4.85 \cdot 10^{-43}$ and $1.80 \cdot 10^{-43}$ [$m^5\ V^{-2}$] for **I** and **II** respectively) and the calculated merit factors ($\chi^{(3)}/\alpha$) ($3.92 \cdot 10^{20}$ and $1.50 \cdot 10^{20}$ [$m^3\ V^{-2}$] for **I** and **II** respectively) clearly bring out that compound (**I**) has a better NLO properties.

It is of interest to note that the obtained results are in line with those found in several recent studies [39–42]. In fact, the comparison of the obtained values and those described in the literature indicates that the third order NLO susceptibilities of the studied compounds are of the same order of magnitude as those used in the NLO applications.

The NLO characterization has also been performed by THG measurements using maker fringes technique. The third order nonlinear optical susceptibility ($\chi^{(3)}_{THG}$) values of the organic–inorganic thin films of the investigated compounds were evaluated by comparing the THG signal with that of the reference material (SiO_2). In our calculations using formula (3), the refractive index of the organic–inorganic thin films was assumed to be the same as that of the fused silica glass substrate. The data were corrected taken into account the air contribution.

The values of the ($\chi^{(3)}_{THG}$) at $\lambda = 1064$ nm range from $0.56 \cdot 10^{-20}$ to $1.68 \cdot 10^{-20}$ [$m^2\ V^{-2}$] (Table 2). These values are two orders of magnitude larger than the $\chi^{(3)}_{THG}$ value of silica, which is the reference material for THG method. One can also notice the good agreement between the results obtained using THG and DFWM techniques. These values are comparable with the one characteristic of other semi-organic materials [21,22].

4. Conclusion

In summary, we have reported here the syntheses, third order nonlinear optical properties, and structural characterization of two new semi-organic compounds containing quinolinium cations. The degenerate four wave mixing (DFWM) measurements at 532 nm, and the third-harmonic generation (THG) results at $\lambda = 1064$ nm, clearly showed that the studied compounds possess not only high third nonlinear optical properties but also important optical limitation properties. The two compounds display different optical behaviours since compound (**I**) has more interesting nonlinear optical properties than compound (**II**). The accurate structural analysis showed clearly that the differences between the two semi-organic compounds are mostly due to the intermolecular interactions and the molecular arrangements rather to than to any anions effect as previously shown in similar semi-organic compounds. The efficiency of the hydrogen-bond interactions is directly related to the donor–acceptor charge transfer and appears to play, by that way, a key role in the net significant enhancement of the third-harmonic generation NLO properties in the semi-organic compounds.

5. Supplementary material

CCDC 670758 and -671321 contain the supplementary crystallographic data for this paper. These data can be obtained free of charge from The Cambridge Crystallographic Data Centre via http://www.ccdc.cam.ac.uk/data_request/cif.

Acknowledgements

The authors would like to thank the Service Commun de Diffraction X sur Monocristaux (Nancy Université) for providing access to crystallographic experimental facilities. Authors are indebted to Professor Dominik Schaniel and to Doctor Pierrick Durand for many helpful discussions.

References

[1] H.S. Nalwa, M. Hanack, G. Pawlowski, M.K. Engel, Chem. Phys. 245 (1999) 17.
[2] C.J. Yang, S.A. Jenekhe, Chem. Mater. 6 (1994) 196.
[3] L.R. Dalton, W.H. Steier, B.H. Robinson, C. Zhang, A. Ren, S. Garner, A. Chen, T. Londergan, L. Irwin, B. Carlson, L. Fifield, G. Phelan, C. Kincaid, J. Amend, A. Jen, J. Mater. Chem. 9 (1999) 1905.
[4] L. Dalton, A. Harper, A. Ren, F. Wang, G. Todorova, J. Chen, C. Zhang, M. Lee, Ind. Eng. Chem. Res. 38 (1999) 8.
[5] H. Ma, A.K.-Y. Jen, L.R. Dalton, Adv. Mater. 14 (2002) 1339.
[6] M. He, T.M. Leslie, J.A. Sinicropi, Chem. Mater. 14 (2002) 2393.
[7] S.S.H. Mao, Y. Ra, L. Guo, C. Zhang, L.R. Dalton, A. Chen, S. Garner, W.H. Steier, Chem. Mater. 10 (1998) 146.
[8] A.W. Harper, S.S.H. Mao, Y. Ra, C. Zhang, J. Zhu, L.R. Dalton, S. Garner, A. Chen, W.H. Steier, Chem. Mater. 11 (1999) 2886.
[9] D. Josse, R. Heirle, I. Ledoux, J. Zyss, Appl. Phys. Lett. 53 (1988) 2251.
[10] B.F. Levine, C.G. Bethea, C.D. Thermond, R.T. Lynch, J.L. Bernstein, J. Appl. Phys. 50 (1979) 2523.
[11] R. Hierle, J. Badan, J. Zyss, J. Cryst. Growth 69 (1984) 545.
[12] A. Ben Ahmed, H. Feki, Y. Abid, H. Boughzala, A. Mlayah, J. Mol. Struct. 888 (2008) 180.
[13] T. Dammak, N. Fourati, Y. Abid, H. Boughzala, A. Mlayah, C. Minot, Spectrochim. Acta A 66 (2007) 1097.
[14] R. Ittyachan, P. Sagayaraj, J. Cryst. Growth 249 (2003) 553.
[15] A. Joseph Arul Pragasam, S. Selvakumar, K. Thamizharasan, D. Premand, P. Sagayaraj, Cryst. Growth 280 (2005) 271.
[16] S. Dhanuskodi, J. Ramajothi, Cryst. Res. Technol. 39 (2004) 592.
[17] M.K. Marchewka, S. Debrusb, A. Pietraszko, A.J. Barnes, H. Ratajczak, J. Mol. Struct. 656 (2003) 265.
[18] S.G. Raja, G.R. Kumar, R. Mohan, S. Pandi, R. Jayavel, J. Mater. Chem. Phys. 90 (2005) 144.
[19] S.S. Terzyan, H.A. Karapetyan, R.B. Sukiasyan, A.M. Petrosyan, J. Mol. Struct. 687 (2004) 111.
[20] D.S. Chemla, J. Zyss, Nonlinear Optical Properties of Organic Molecules and Crystals, vols. 1–2, Academic Press, New York, 1987.
[21] K. Bouchouit, Z. Sofiani, B. Derkowska, S. Abed, N. Benali-cherif, M. Bakasse, B. Sahraoui, Opt. Commun. 278 (2007) 180.
[22] K. Bouchouit, Z. Essaidi, S. Abed, A. Migalska-Zalas, B. Derkowska, N. Benali-cherif, M. Mihaly, A. Meghea, B. Sahraoui, Chem. Phys. Lett. 455 (2008) 270.
[23] R. Hooft. Collect. Nonius BV, Delft, The Netherlands, 1998.
[24] Z. Otwinowski, W. Minor, Methods Enzymol. 276 (1996) 307.
[25] G.T. DeTitta, J. Appl. Crystallogr. 18 (1985) 75.
[26] G.M. Sheldrick, Acta Cryst. A 64 (2008) 112.
[27] L.J. Farrugia, J. Appl. Cryst. 32 (1999) 837.
[28] B. Sahraoui, G. Rivoire, Opt. Commun. 138 (1997) 109.
[29] R.W. Boyd, Nonlinear Optics, second ed., Academic, New York, 2003.
[30] B. Derkowska, M. Wojdyla, R. Czaplicki, Z. Sofiani, W. Bala, B. Sahraoui, Opt. Commun. 274 (2007) 206.
[31] D. Maker, R.W. Terhune, M.F. Niseno, C.M. Savage, Phys. Rev. Lett. 8 (1962) 21.
[32] U. Gubler, C. Bosshard, Phys. Rev. B 16 (2000) 10702.
[33] F. Kajzar, J. Messier, Phys. Rev. A 32 (1985) 2352.
[34] W. Kautek, J. Kruger, M. Lenzner, S. Srtania, C. Spielmann, F. Krausz, App. Phys. Lett. 69 (1996).
[35] M.N. Burnett, C.K. Johnson, ORTEPIII, Report ORNL-6895, Oak Ridge National Laboratory, Tennessee, USA, 1996.
[36] J.E. Davies, A.D. Bond, Acta Cryst. E 57 (2001) 47.
[37] T.V. Sundar, V. Parthasarathi, S. Thamotharan, K.G. Sekar, Acta Cryst. E 59 (2003) 327.
[38] E.E. Bendeif, S. Dahaoui, N. Benali-Cherif, C. Lecomte, Acta Cryst. B 63 (2007) 448.
[39] B. Sahraoui, I.V. Kityk, I. Fuks, B. Paci, P. Baldeck, J.-M. Nunzi, P. Frere, J. Roncali, J. Chem. Phys. 115 (2001) 6179.
[40] B. Sahraoui, R. Chevalier, X. Nguyen Phu, G. Rivoire, J. Appl. Phys. 80 (1996) 4854.
[41] B. Sahraoui, G. Rivoire, J. Zaremba, N. Terkia-Derdra, M. Sallé, J. Opt. Soc. Am. B 15 (1998) 923.
[42] A. Migalska-Zalas, J. Luc, B. Sahraoui, I.V. Kityk, Opt. Mater. 28 (2006) 1147.